Theory of Elasticity of Amorphous Networks: Effect of Constraints along Chains

Burak Erman

School of Engineering, Bogazici University, Bebek, 80815, Istanbul, Turkey

Lucien Monnerie*

Laboratoire de Physico-Chimie Structurale et Macromolêculaire, Associê au CNRS, ESPCI, 10 rue Vauquelin, 75231 Paris Cedex 05, France. *Received July 18, 1988; Revised Manuscript Received February 2, 1989*

ABSTRACT: The constrained junction model of amorphous polymeric networks is modified to include constraints along the chain contours. The elastic free energy ΔA_{el} is calculated as $\Delta A_{el} = \Delta A_{ph} + \Delta A_c$, where ΔA_{ph} is the contribution from the phantom network and ΔA_c is due to the effects of constraints or entanglements along the network chains. ΔA_{ph} is proportional to the cycle rank ξ while ΔA_c is proportional to the number of chains. The effect of constraints is represented by a single parameter κ_G in the present treatment instead of the two parameters κ and ζ of the constrained junction model. Results of calculations indicate that the predictions of the present model differ from those of the constrained junction model in two important respects: (i) According to the present model the small strain moduli may obtain values above those predicted by the affine network model. The latter forms an upper bound for the constrained junction treatment. (ii) The dependence of moduli on extension and swelling is more sensitive than that predicted by the constrained junction model. These two differences improve agreement of the theory with experimental data as presented in the following two papers.

Introduction

A phantom network model constitutes a convenient starting point for statistical mechanical theories of real networks. The structure and properties of phantom networks are well understood.[1-11] They consist of chains that may pass freely through each other while fluctuating about their time-averaged positions. In this sense, the effects of entanglements resulting from the exclusion of volume of a chain to others due to the topological connectivity of the network are missing. Corrections for the effects of entanglements form the basis of various current molecular theories of rubber elasticity.[11,12]

According to the model introduced by Flory,[14] the deviation of a real network from the phantom network model results from constraints affecting the fluctuations of junctions. Thus, according to this model, which has subsequently been termed as the constrained junction model, the junctions are chosen as structural members affected directly by entanglements. The fact that this is an approximation to the real picture where entanglements are operative, diffusely, along the chains have been emphasized.[14] Transformation of points along the chains does not appear explicitly in the formulation of the constrained junction theory, however.

In the present study we modify the constrained junction model by considering the action of constraints at points along the chains between junction points. Results of calculations presented below and their comparison with experimental data in the following two papers[16,17] indicate that the present formulation constitutes a further improvement over the constrained junction model.

In the first section below, we give a brief review of the phantom and constrained junction models. For more detailed information, the reader is referred to ref 5-11, 14, and 15. In the next section we derive the elastic free energy of a network whose chains are affected by constraints. The relationship of stress to strain is derived in the third section, followed by numerical calculations and a comparison of the present treatment with results of the constrained junction model.

Review of Phantom and Constrained Junction Models

The instantaneous configuration of a chain in a phantom network is depicted by the heavy line A_1A_{n+1} in Figure 1. Let us consider a given chain connected to ϕ-functional junctions ($\phi = 3$ in the figure) at its extremities. Points $\overline{A_1}$ and $\overline{A_{n+1}}$ are the mean positions of the junctions A_1 and A_{n+1}, respectively. The chain is subdivided into n Gaussian subchains. Two consequtive points A_i and A_{i+1} along the chain denote the end points of the ith subchain where $1 \le i \le n$. The vectors $\Delta\mathbf{R}_i$ represent the instantaneous fluctuations of points A_i from their mean locations $\overline{A_i}$ in the phantom network. All $\overline{A_i}$ lie on the line $\overline{A_1A_{n+1}}$. The vector from $\overline{A_1}$ to $\overline{A_{n+1}}$ defines the time-averaged end-to-end vector $\bar{\mathbf{r}}_{ph}$ in the phantom network. The instantaneous end-to-end vector $\mathbf{r}$ extends from A_1 to A_{n+1}. For the ensemble of chains over the whole network, $\bar{\mathbf{r}}_{ph}$ and $\mathbf{r}$ have Gaussian distributions.

In a phantom network in the state of rest, the following relations exist[6-10] among the quantities $\langle \bar{x}_{ph}^2 \rangle_0$, $\langle (\Delta X_i)^2 \rangle_0$, and $\langle x^2 \rangle_0$:

$$\langle \bar{x}_{ph}^2 \rangle_0 = (1 - 2/\phi)\langle x^2 \rangle_0$$

$$\langle (\Delta X_i)^2 \rangle_0 = \left[\frac{\phi - 1}{\phi(\phi - 2)} + \frac{\theta(1-\theta)(\phi - 2)}{\phi} \right] \langle x^2 \rangle_0 \quad (1)$$

Here, $\bar{x}_{ph}$, ΔX_i, and x are the x components of $\bar{\mathbf{r}}_{ph}$, $\Delta\mathbf{X}_i$, and $\mathbf{r}$. The angular brackets denote the ensemble average, the subscript 0 indicates the state of reference, and

$$\theta = (i - 1)/n \quad (2)$$

indicates the position of the end point A_i between the ith and $(i + 1)$th subchains, expressed as a fraction of the chain contour length between two junctions. Expressions similar to eq 1 may be written for the y and z components. That the problem may be treated separately in terms of components follows the Gaussian character of the chains. In the present study only the x components will be indicated.

Under macroscopic deformation, represented by the principal extension ratios λ_x, λ_y, and λ_z, the components $\langle \bar{x}_{ph}^2 \rangle$ of the mean chain vectors transform affinely:

$$\langle \bar{x}_{ph}^2 \rangle = (1 - 2/\phi)\lambda_x^2 \langle x^2 \rangle_0 \quad (3)$$

According to the theory developed independently by Pearson[6] and Ullman,[7,8] the fluctuations of the end points of subchains are independent of macroscopic deformation.

0024-9297/89/2222-3342$01.50/0

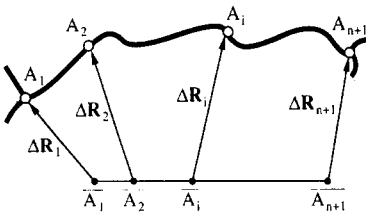

Figure 1. Instantaneous configuration of a phantom network chain shown by the heavy line. A_1 and A_{n+1} are the junctions. The chain is divided into n Gaussian subchains. End points of the subchains along A_1A_{n+1} are designated by A_t-$\overline{A_1}$, ..., $\overline{A_{n+1}}$ denote the time-averaged positions of A_i, ..., A_{n+1} in the phantom network. $\Delta\mathbf{R}_i$ indicates the instantaneous fluctuation of point A_i from its average location $\overline{A_i}$.

Thus the second term of eq 1 continues to hold also in the deformed state. This conclusion is based on the original treatment of James,[1] where the end points of subchains are treated as junctions in the partition function of the network. An alternate approximate treatment[9,10] shows that if only the multifunctional junctions are retained in the partition function matrix and if the network chains are assumed to consist of n freely jointed Gaussian subchains, both in the undeformed and deformed states, then $\langle(\Delta X_i)^2\rangle$ depend on macroscopic deformation according to the following relation:

$$\langle(\Delta X_i)^2\rangle_0 = \left[\frac{\phi - 1}{\phi(\phi - 2)} + \frac{\theta(1-\theta)(\phi-2)}{\phi}\lambda_x^2\right]\langle x^2\rangle_0 \qquad (4)$$

This expression reduces to that of the Pearson–Ullman expression only at the multifunctional junctions, i.e., when $\theta = 0$ or 1.

The extent of the constraints operating on network chain points depends on the type of the phantom network model chosen as reference. In the following we develop the theory of constraints in terms of both of the phantom network models stated above. For brevity, we term the formulation based on the phantom network with strain-independent fluctuations of chain points as the "constrained chain" model, or simply the CC model. Similarly, we term the formulation based on the phantom network with strain-dependent fluctuations of chain points as the "modified constrained chain" model, or simply the MCC model.

The elastic free energy ΔA_{ph} of a phantom network is given as

$$\Delta A_{ph} = \tfrac{1}{2}\xi kT\sum_t(\lambda_t^2 - 1) \qquad t = x, y, z \qquad (5)$$

where ξ is the cycle rank[5] of the network indicating the number of independent cyclic paths in the connected structure of the phantom network.

The elastic free energy ΔA_{el} of the constrained junction model is given[14,15] as

$$\Delta A_{el} = \Delta A_{ph} + \Delta A_c \qquad (6)$$

Here ΔA_c serves as the correction to the phantom network approximation and is given by the constrained junction theory as

$$\Delta A_c = \tfrac{1}{2}\mu kT\sum_t[B_t + D_t - \ln(1 + B_t) - \ln(1 + D_t)] \qquad (7)$$

where μ is the number of junctions and

$$B_t = \kappa^2(\lambda_t^2 - 1)(\lambda_t^2 + \kappa)^{-2}$$

$$D_t = \lambda_t^2 B_t/\kappa \qquad (8)$$

The parameter κ in eq 8 is defined as

$$\kappa = \langle(\Delta R)^2\rangle_0/\langle(\Delta s)^2\rangle_0 \qquad (9)$$

where $\langle(\Delta R)^2\rangle_0$ is the mean-squared fluctuations of junctions in the reference state of the phantom network. Each junction in the real network is assumed to be under the effect of constraints resulting from the material properties of the chains that interpenetrate densely in the amorphous bulk structure. $\langle(\Delta s)^2\rangle_0$ in eq 9 represents the mean-squared fluctuations of junctions from their mean positions in the reference state under the action of constraints only. For a phantom network, in which there are no constraints by definition, $\langle(\Delta s)^2\rangle_0$ is unbounded and κ equates to zero. In this case the term ΔA_c vanishes, as expected. If the constraints are infinitely strong, $\langle(\Delta s)^2\rangle_0$ is zero and κ goes to infinity. This corresponds to the affine network model. ΔA_{el} for the affine network forms the upper limit to the elastic free energy of the constrained junction model. In this limit, $B_t = \lambda_t^2 - 1$ and $D_t = 0$. Use of these with eq 7 in eq 6 leads to the total elastic free energy ΔA_{af} of an affine network as

$$\Delta A_{af} = \tfrac{1}{2}(\xi + \mu)kT\sum_t(\lambda_t^2 - 1) - \mu kT\ln(\lambda_x\lambda_y\lambda_z) \qquad (10)$$

The elastic free energy for the constrained junction model lies between ΔA_{ph} given by eq 5 and ΔA_{af} given by eq 10. At low deformations the effects of constraints are strong and the elastic free energy is closer to that given by eq 10. At high deformations or high degrees of swelling, the elastic free energy approaches that of the phantom network.

The predictions of the constrained junction theory reflect, qualitatively, several properties of real networks. With the introduction[15] of a second parameter ζ, results of stress–strain experiments may be predicted quantitatively[18] by the theory. The second parameter is necessitated by experimental observations where the moduli of networks decrease much faster by extension or swelling than that predicted with the κ parameter only. In this sense the introduction of ζ leads to significant improvement in agreement between theory and experiment. Its relation to molecular parameters is not as clear as that of the κ parameter, however.

Effects of Constraints along Network Chains: The CC and MCC Models

The chains in an amorphous polymeric network are densely entangled with their neighbors. Points along the chains cannot therefore assume all of the configurations available to them in the absence of such entanglements as obtained in the phantom network analogue. This effect of entanglements obviously results in the reduction of the number of configurations available to each chain of the phantom network. Following Flory,[14] we make the assertion that only the entanglements that are affected by deformation contribute to the modulus. Such entanglements, which operate at all points along the chain, are assumed to diminish with increasing tension or swelling. This assumption is motivated by the argument that extension along a given direction should allow for more freedom for fluctuations in that direction.

Introduction of strain-dependent constraints in the manner stated above is therefore expected to modify the instantaneous distribution of the mass centers of chains relative to their locations in the phantom network. Directing attention to the instantaneous distribution of the mass centers of chains may be regarded as a generalization of the constrained junction model. In the latter, the effects of constraints on the instantaneous distribution of junction positions relative to those obtained in the phantom network were considered in deriving the elastic free energy.

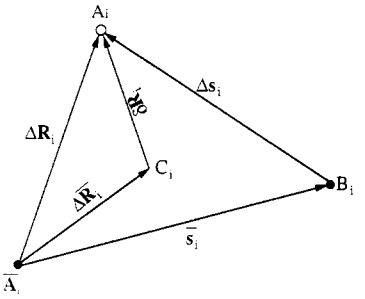

Figure 2. Instantaneous and mean positions of the chain point A_i in the absence and presence of constraints (see text for definition of the various symbols).

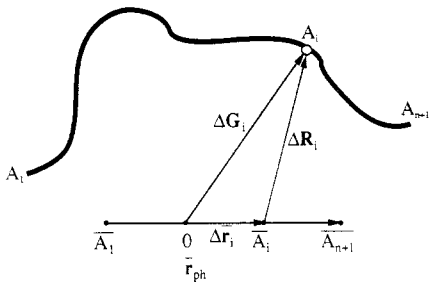

Figure 3. Position of point A_i relative to the midpoint of $\bar{\mathbf{r}}_{ph}$.

Inclusion of the constraints on junctions only was assumed[14,15] to be representative of the action of all entanglements. In this section we derive the elastic free energy due to constraints operating at the end points of each Gaussian subchain. The choice of these points as centers affected by constraints may seem to be arbitrary due to the fact that the number of Gaussian subchains in a given chain is not well defined. The following calculations show, however, that the results are not critically dependent on the number of Gaussian subchains. The consideration of the end points of Gaussian subchains instead of the junctions only thus forms the basic modification from the constrained junction model.

The instantaneous position of point A_i is depicted in Figure 2. $\Delta\mathbf{R}_i$ is the instantaneous fluctuation of point A_i from its mean position $\bar{A}_i$ in the phantom network. $\bar{\mathbf{s}}_i$ locates the position of B_i, which is the mean position of point A_i that would be obtained under the action of constraints only. $\Delta\mathbf{s}_i$ is the instantaneous fluctuation of A_i from point B_i. Under the joint action of the phantom network and the constraints, the mean position of A_i moves to point C_i, identified by the vector $\overline{\Delta\mathbf{R}_i}$ relative to $\bar{A}_i$. $\delta\mathbf{R}_i$ represents the instantaneous fluctuation of A_i from point C_i.

The transformations of $\Delta\mathbf{R}_i$ are given either by eq 1 (CC model) or by eq 4 (MCC model). The transformations of the vectors $\bar{\mathbf{s}}_i$ and $\Delta\mathbf{s}_i$ may be assumed to be affine in analogy with the constrained junction model.

In the phantom network, the instantaneous position of point A_i from the midpoint O of $\bar{\mathbf{r}}_{ph}$ is shown in Figure 3 by the vector $\Delta\mathbf{G}_i$. It is related to $\Delta\mathbf{R}_i$ by

$$\Delta\mathbf{G}_i = \Delta\mathbf{R}_i + \Delta\bar{\mathbf{r}}_i \tag{11}$$

where $\Delta\bar{\mathbf{r}}_i$ denotes the vector from the midpoint O to the time-averaged position of point A_i in the phantom network. The instantaneous fluctuation $\Delta\mathbf{R}_G$ of the mass center of the chain from its average location O in the phantom network is shown in Figure 4. $\Delta\mathbf{R}_G$ may be related to $\Delta\mathbf{G}_i$ by

$$(\Delta\mathbf{R}_G)^2 = \frac{1}{n+1}\sum_{i=1}^{n+1}\Delta\mathbf{G}_i\cdot\Delta\mathbf{G}_i \tag{12}$$

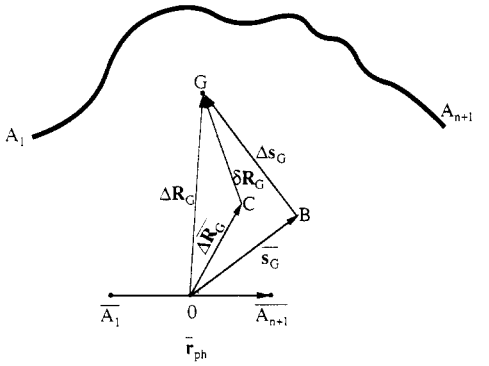

Figure 4. Position of the instantaneous mass center G of the chain (see text for definition of the various symbols).

Substituting eq 11 into eq 12 and taking the ensemble average lead to

$$\langle(\Delta\mathbf{R}_G)^2\rangle = \frac{1}{n+1}\sum_{i=1}^{n+1}[\langle(\Delta\mathbf{R}_i)^2\rangle + \langle(\Delta\bar{\mathbf{r}}_i)^2\rangle] \tag{13}$$

where the terms $\langle\Delta\mathbf{R}_i\cdot\Delta\bar{\mathbf{r}}_i\rangle$ have been equated to zero inasmuch as fluctuations and mean vectors are uncorrelated in the phantom network.[10] The quantity θ given by eq 2, which defines the position of A_i along the chain contour, also describes the position of $\bar{A}_i$ along $\bar{\mathbf{r}}_{ph}$, leading to the following expression:

$$\Delta\bar{\mathbf{r}}_i = (\theta - \tfrac{1}{2})\bar{\mathbf{r}}_{ph} \tag{14}$$

Squaring eq 14, taking the ensemble average, and substituting into eq 13, together with eq 1 for the CC model or with eq 4 for the MCC model, lead to, in terms of x components

$$\langle(\Delta X_G)^2\rangle = [1 + (\lambda^2 - 1)\Phi]\frac{\langle x^2\rangle_0}{4(1 - 2/\phi)} \tag{15}$$

where ΔX_G represents the x component of $\Delta\mathbf{R}_G$ and

$$\Phi = \left(1 - \frac{2}{\phi}\right)^2\left(\frac{1}{3} + \frac{2}{3n}\right) \quad \text{for CC model}$$

$$\Phi = (1 - 2/\phi)^2 \quad \text{for MCC model} \tag{16}$$

It is worth noting that only the CC model results in an n-dependent value for $\langle(\Delta X_G)^2\rangle$. In the undeformed state the difference between the CC and the MCC models vanishes, leading to $\langle(\Delta X_G)^2\rangle_0 = \langle x^2\rangle_0/4(1 - 2/\phi)$. For a tetrafunctional network, for example, the mean-squared fluctuations of mass centers of chains about point O equate to one-half of the mean-square end-to-end chain length. It is worth noting that the fluctuations of junctions in a tetrafunctional phantom network is $^3/_8$ times the mean-square chain length.

Consideration of the effects of constraints separately on each point A_i as shown in Figure 2 may further be simplified by reformulating the problem in terms of the constraints affecting the instantaneous position of the chain mass center. The latter situation is shown in Figure 4. $\Delta\mathbf{R}_G$ denotes the instantaneous position of the mass center of the chain from point O. (Point O is the mean position of the center of mass of this given chain in the phantom network.) Point B located by the vector $\bar{\mathbf{s}}_G$ from point O represents the mean position of the center of mass of the chain under only the effect of constraints that act along the considered chain including the end points which are junctions. In this respect point B may also be considered as the centroid of all points B_i (described in Figure 2) for the given chain. $\Delta\mathbf{S}_G$ denotes the instantaneous position

of point G relative to point B. Point C is the new position that the mass center will be disposed about under the combined effect of phantom network and the constraints. $\Delta\overline{\mathbf{R}_G}$ locates the position of point C relative to O and $\delta\mathbf{R}_G$ denotes the instantaneous location of the chain mass center relative to point C.

The distribution of the variables $\Delta\mathbf{R}_G$, $\overline{\mathbf{s}_G}$, $\Delta\mathbf{s}_G$, $\Delta\overline{\mathbf{R}_G}$, and $\delta\mathbf{R}_G$ will be assumed to be Gaussian. The distribution functions are expressed in terms of the x components of the variables as

$$R(\Delta X_G) = (\rho_\lambda/\pi)^{1/2} \exp[-\rho_\lambda(\Delta X_G)^2]$$

$$H(\overline{x_G}) = (\eta_\lambda/\pi)^{1/2} \exp[-\eta_\lambda\overline{x_G}^2]$$

$$S(\Delta x_G) = (\sigma_\lambda/\pi)^{1/2} \exp[-\sigma_\lambda(\Delta x_G)^2]$$

$$\Theta(\Delta\overline{X_G}) = (\theta_\lambda/\pi)^{1/2} \exp[-\theta_\lambda(\Delta\overline{X_G})^2]$$

$$P(\delta X_G) = [(\rho_\lambda + \sigma_\lambda)/\pi]^{1/2} \exp[-(\rho_\lambda + \sigma_\lambda)(\delta X_G)^2] \quad (17)$$

where the parameters ρ_λ, η_λ, σ_λ, and θ_λ are given as

$$\rho_\lambda = 1/2\langle(\Delta X_G)^2\rangle$$

$$\eta_\lambda = 1/2\langle\overline{x_G}^2\rangle$$

$$\sigma_\lambda = 1/2\langle(\Delta x_G)^2\rangle$$

$$\theta_\lambda = 1/2\langle(\Delta\overline{X_G})^2\rangle \quad (18)$$

The subscript λ implies that these variables are in general functions of deformation. The notation of eq 17 is chosen to be identical with that of the constrained junction theory to facilitate comparison. The last of eq 17 follows from the condition of combined action of phantom network and constraint effects.

The instantaneous distribution of the components ΔX_G in the deformed network is given by the convolution of $P(\delta X_G)$ and $\Theta(\Delta\overline{X_G})$:

$$R_*(\Delta X_G) = \int P(\delta X) \times \Theta(\Delta\bar{X})\, d\Delta\bar{X} \quad (19)$$

The subscript asterisk denotes the difference of the distribution function of ΔX_G in the real network from the a priori probability $R(\Delta X_G)$ in the phantom network. The distribution function $R_*(\Delta X_G)$ is given as

$$R_*(\Delta X_G) = (\rho_{*\lambda}/\pi)^{1/2} \exp[-\rho_{*\lambda}(\Delta X_G)^2] \quad (20)$$

Substituting from eq 17 into eq 19 and performing the integration lead to the following expression for $\rho_{*\lambda}$:

$$\frac{\rho_\lambda}{\rho_{*\lambda}} = 1 + \left(\frac{\sigma_\lambda}{\rho_\lambda}\right)\frac{[(\sigma_\lambda/\rho_\lambda)(\rho_\lambda\eta_\lambda^{-1} - 1) - 1]}{(1 + \sigma_\lambda/\rho_\lambda)^2} \quad (21)$$

In the undeformed state $R_*(\Delta X_G)$ should reduce to $R(\Delta X_G)$. Representing the parameters σ_λ, ρ_λ, and η_λ, respectively, by σ_0, ρ_0, and η_0 when $\lambda = 1$, the condition that $R_*(\Delta X_G) \equiv R(\Delta X_G)$ in the undeformed state is obtained from eq 21 as

$$\eta_0^{-1} = \rho_0^{-1} + \sigma_0^{-1} \quad (22)$$

Substituting eq 22 into eq 21 leads to

$$\frac{\rho_\lambda}{\rho_{*\lambda}} = 1 + \frac{\left(\frac{\sigma_\lambda}{\rho_\lambda}\right)^2\left(\frac{\eta_0}{\eta_\lambda} - 1\right) + \left(\frac{\sigma_\lambda}{\rho_\lambda}\right)\left[\left(\frac{\eta_0}{\eta_\lambda}\right)\left(\frac{\sigma_\lambda}{\sigma_0}\right) - 1\right]}{\left(1 + \frac{\sigma_\lambda}{\rho_\lambda}\right)^2} \quad (23)$$

The details of calculations are not indicated inasmuch as they follow exactly from those given in ref 15.

The distribution of the components Δx_G in the deformed network is given, similarly, by

$$S_*(\Delta x_G) = (\sigma_{*\lambda}/\pi)^{1/2} \exp[-\sigma_{*\lambda}(\Delta x_G)^2] \quad (24)$$

where $\sigma_{*\lambda}$ is defined by[15]

$$\frac{\sigma_\lambda}{\sigma_{*\lambda}} = 1 + \left(\frac{\sigma_\lambda}{\rho_\lambda}\right)^{-1}\left(\frac{\rho_\lambda}{\rho_{*\lambda}} - 1\right) \quad (25)$$

We introduce a parameter κ_G, in a manner identical with the κ parameter of the constrained junction model, as

$$\kappa_G = \sigma_0/\rho_0 = \langle(\Delta X_G)^2\rangle_0/\langle(\Delta x_G)^2\rangle_0 \quad (26)$$

The correspondence of the physics behind κ and κ_G is obvious.

It was stated above that the vectors $\overline{\mathbf{s}_i}$ and $\Delta\mathbf{s}_i$ may be assumed to be affine in macroscopic deformation. The same assumption may be made for the vectors $\Delta\mathbf{s}_G$ and $\overline{\mathbf{s}_G}$. Thus

$$\sigma_\lambda/\sigma_0 = \lambda_x^{-2}$$

$$\eta_0/\eta_\lambda = \lambda_x^2 \quad (27)$$

Writing $\sigma_\lambda/\rho_\lambda = (\sigma_\lambda/\sigma_0)(\sigma_0/\rho_0)(\rho_0/\rho_\lambda)$ and using eq 15, 26, and 27, we obtain following expression for the ratio $\sigma_\lambda/\rho_\lambda$:

$$\sigma_\lambda/\rho_\lambda = \lambda^{-2}\frac{\kappa_G}{1 + (\lambda_x^2 - 1)\Phi} \equiv \lambda^{-2}h(\lambda_x) \quad (28)$$

where

$$h(\lambda_x) = \kappa_G[1 + (\lambda_x^2 - 1)\Phi]^{-1} \quad (29)$$

The difference between the CC and MCC models arises from the definition of Φ given by eq 16.

Substituting eq 27 and 28 into eq 23 and 25 and defining two new variables B_x and D_x (similar to those of the constrained junction theory) as

$$B_x = \frac{\rho_\lambda}{\rho_{*\lambda}} - 1 \qquad D_x = \frac{\sigma_\lambda}{\sigma_{*\lambda}} - 1 \quad (30)$$

we obtain

$$B_x = h(\lambda_x)^2(\lambda_x^2 - 1)/[\lambda_x^2 + h(\lambda_x)]^2 \quad (31)$$

$$D_x = \lambda_x^2 B_x/h(\lambda_x) \quad (32)$$

Similar expressions follow for the y and z components. Comparison of eq 31 and 32 with the corresponding expressions of the constrained junction model shows that κ of the latter is replaced by the function $h(\lambda_x)$.

Following the arguments of ref 14 and 15, the expression for the elastic free energy due to constraints is obtained as

$$\Delta A_c = \frac{\nu kT}{2}\sum_t[B_t + D_t - \ln(1 + B_t) - \ln(1 + D_t)] \quad (33)$$

It should be noted that in the present formulation the ΔA_c is due to the total effect of ν chains, whereas in the constrained junction theory it is due to the total effect of μ junctions.

The total elastic free energy of the network is obtained by substituting eq 5 and 33 into eq 6 as

$$\Delta A_{el} = \tfrac{1}{2}\xi kT\sum_t\{\lambda_t^2 - 1 + (\nu/\xi)[B_t + D_t - \ln(1 + B_t) - \ln(1 + D_t)]\} \quad (34)$$

For the phantom network $\kappa_G = 0$ from the definition given by eq 26. In this limit $B_t = D_t = 0$, and eq 34 reduces to the elastic free energy of the phantom network. When the

effect of constraints is infinitely large, $\kappa_G \to \infty$. In this limit

$$B_t = \lambda_t^2 - 1 \qquad D_t = 0 \tag{35}$$

$$\Delta A_{el} = \tfrac{1}{2}(\xi + \nu)kT\sum_t(\lambda_t^2 - 1) - \nu kT \ln (\lambda_x\lambda_y\lambda_z) \tag{36}$$

The product $\lambda_x\lambda_y\lambda_z$ is unity when the volume of the network is the same as that in the state of reference. Comparing eq 10 and 36 and considering that $\nu = \mu\phi/2$, lead to the conclusion that

$$\lim_{\kappa_G \to \infty} \Delta A_{el} > \Delta A_{af} \tag{37}$$

Stress-Strain Relations and Numerical Calculations

The tth principal component τ_t of stress (force per unit deformed area) is given[14] as

$$\tau_t = 2V^{-1}\lambda_t^2(\partial\Delta A_{el}/\partial\lambda_t^2) \tag{38}$$

where V is the volume of the network in the final state. The derivative of the elastic free energy is obtained from eq 34 as

$$\frac{\partial\Delta A_{el}}{\partial\lambda_t^2} = \frac{1}{2}\xi kT\left\{1 + \frac{\nu}{\xi}[B\dot{B}(1 + B)^{-1} + D\dot{D}(1 + D)^{-1}]_t\right\} \tag{39}$$

where

$$\dot{B} = \frac{\partial B}{\partial\lambda^2} = B\left[(\lambda^2 - 1)^{-1} - 2(\lambda^2 + h)^{-1} - 2\frac{h\lambda^2\Phi}{\kappa_G(\lambda^2 + h)}\right] \tag{40}$$

$$\dot{D} = \frac{\partial D}{\partial\lambda^2} = B\left[h^{-1} + \frac{\lambda^2\Phi}{\kappa_G}\right] + \frac{\lambda^2\dot{B}}{h} \tag{41}$$

where $h = h(\lambda^2)$ is used for brevity. If Φ is set equal to zero and $\kappa_G = \kappa$, then $h = \kappa$ and the expressions for B, D, $\dot{B}$, and $\dot{D}$ reduce to those given by the constrained junction theory. Defining $K(\lambda^2)$ as

$$K(\lambda^2) = \frac{B\dot{B}}{1 + B} + \frac{D\dot{D}}{1 + D} \tag{42}$$

the expression for the stress may be written as

$$\tau_t = \frac{\xi kT}{V}\lambda_t^2\left[1 + \frac{\nu}{\xi}K(\lambda_t^2)\right] \tag{43}$$

The state of deformation for simple tension or compression is given as

$$\lambda_x = \left(\frac{V}{V_0}\right)^{1/3}\alpha = \left(\frac{v_{2c}}{v_2}\right)^{1/3}\alpha$$

$$\lambda_y = \lambda_z = \left(\frac{v_{2c}}{v_2}\right)^{1/3}\alpha^{-1/2} \tag{44}$$

where v_{2c} is the volume fraction of polymer in the reference state which may conveniently be chosen as the state of formation of the network. v_2 is the volume fraction of network during the experiment, and α is the ratio of the final length to the initial undistorted length when the volume fraction is v_2. The total force f acting on the sample at an elongation of α is obtained[14] as

$$f = \frac{\xi kT}{L_0}\left(\frac{v_{2c}}{v_2}\right)^{1/3}\left\{\alpha - \alpha^{-2} + \left(\frac{\nu}{\xi}\right)[\alpha K(\lambda_x^2) - \alpha^{-2}K(\lambda_y^2)]\right\} \tag{45}$$

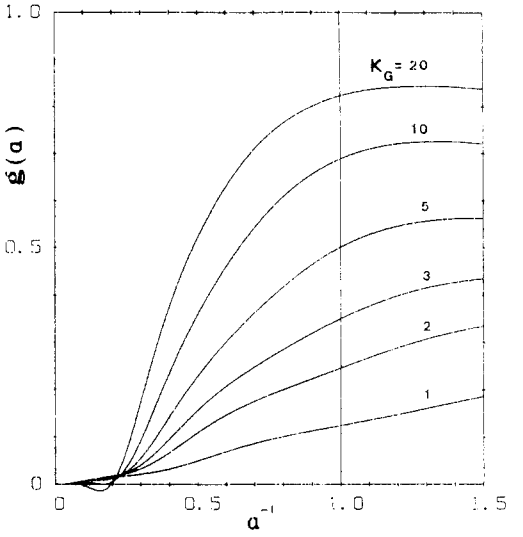

Figure 5. Variation of the strain-dependent part $g(\alpha)$ of the reduced force with α^{-1}. Curves are obtained with the CC model for $v_2 = v_{2c} = 1$.

Here L_0 is the length of the sample in the reference state. The reduced force $[f^*]$ commonly adopted for interpretation of experimental data is defined as

$$[f^*] = \frac{f v_2^{1/3}}{A_d(\alpha - \alpha^{-2})} \tag{46}$$

where A_d is the cross-sectional area in the dry state. Substituting eq 45 into eq 46 leads to

$$[f^*] = [f^*]_{ph}\{1 + (\nu/\xi)[\alpha K(\lambda_x^2) - \alpha^{-2}K(\lambda_y^2)]/(\alpha - \alpha^{-2})\} \tag{47}$$

where $[f^*]_{ph} = (\xi kT/V_d)v_{2c}^{2/3}$ is the phantom modulus and V_d is the volume of the sample in the dry state. The second term in brackets represents the contribution of the constraints to the reduced force, or the modulus. In the limit as $\kappa_G \to \infty$, the reduced force is

$$\lim_{\kappa_G \to \infty}[f^*] = \left(\frac{\xi kT}{V_d}\right)v_{2c}^{2/3}\left(1 + \frac{\nu}{\xi}\right) \tag{48}$$

Substituting the expression $\nu = \xi(1 - 2/\phi)^{-1}$ for a phantom network into eq 48 leads to

$$\lim_{\kappa_G \to \infty}[f^*] = 2\frac{(\phi - 1)}{(\phi - 2)}[f^*]_{ph} \tag{49}$$

where $[f^*]_{ph}$ denotes the network phantom modulus.

For convenience, we define the strain-dependent part of the reduced force of eq 47 by the function $g(\alpha)$ as

$$g(\alpha) = [\alpha K(\lambda_x^2) - \alpha^{-2}K(\lambda_y^2)]/(\alpha - \alpha^{-2}) \tag{50}$$

Dependence of $g(\alpha)$ on α^{-1} is presented in Figures 5–7. In Figure 5, the curves show results for various values of κ_G obtained by the CC model for $v_2 = v_{2c} = 1$. Inasmuch as the number of Gaussian subchains in ordinary network chains is much larger than unity, the term $2/3n$ in eq 16 is equated to zero in the calculations. Values of $g(\alpha)$ calculated for various values of n but not reported in this work show that dependence on n is insignificant for $n > 10$. Results obtained by the MCC model are presented in Figure 6. The effect of swelling for $\kappa_G = 10$ is presented for both the CC (solid curves) and MCC (dashed curves) models in Figure 7. Comparison of these figures indicates that the two models lead to results that are indistinguishable in the compression region, $\alpha^{-1} > 1$. In the tension region, the function $g(\alpha)$ for the MCC scheme shows more

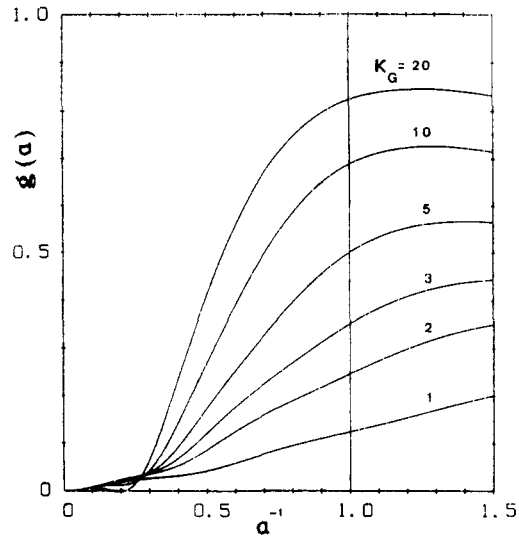

Figure 6. Variation of the strain-dependent part $g(\alpha)$ of the reduced force with α^{-1}. Curves are obtained with the MCC model for $v_2 = v_{2c} = 1$.

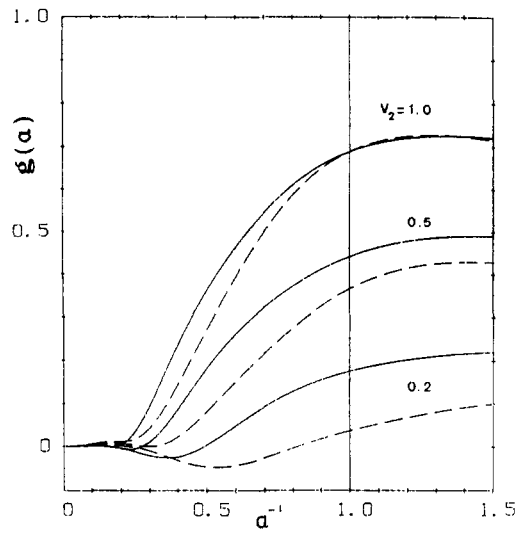

Figure 7. Variation of $g(\alpha)$ with swelling for the CC (solid curves) and MCC (dashed curves) models, for $\kappa_G = 10$.

sensitive dependence on α and swelling. Comparison of Figures 5 and 6 with similar results obtained for the constrained junction model in previous studies[14,15] shows that the present treatment leads to more sensitive dependence of $g(\alpha)$ on extension and swelling.

In the present treatment the elastic free energy due to constraints is obtained by summing over the ν chains whereas in the constrained junction model summation is performed over the μ junctions. This results in a different expression for the reduced force (eq 47) where the term ν/ξ has to be replaced by μ/ξ for the latter. To compare the strain and swelling dependence of the two theories, we choose values of κ_G and κ such that the same value of $[f^*]/[f^*]_{ph}$ is obtained at $\alpha = 1$. Results of calculations performed on this basis for a tetrafunctional network ($\mu/\xi = 1$, $\nu/\xi = 2$) are shown in Figure 8, for $v_2 = 1$ and 0.2. The solid curves are obtained for the CC model with $\kappa_G = 2.95$. The dashed curves are for the constrained junction model with $\kappa = 10$. The present treatment shows stronger dependence on strain and swelling. This feature seems to be a closer representation of experimental data obtained for various elastomeric networks. Introduction of the ζ parameter into the calculations for the constrained junction model leads to stronger dependence on strain and swelling as shown in previous work.[15]

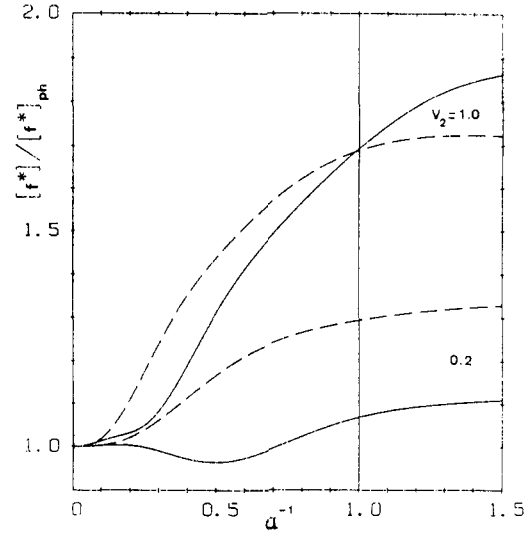

Figure 8. Comparison of $[f^*]/[f^*]_{ph}$ values for the constrained junction model (dashed lines) with the CC model (solid lines) for $v_2 = 1$ and 0.2. κ and κ_G are chosen as 10 and 2.95, respectively.

Conclusions

The present model shows mainly two important differences from the constrained junction theory. First, the adoption of the chain points as being affected by constraints rather than the junctions only leads to elastic free energy and modulus values that may exceed those for an affine network model. Second, the dependence of the modulus on elongation and swelling is more sensitive than that given by the constrained junction theory. Such a dependence, as observed in experiments, is obtained in the present treatment through a single parameter κ_G, whereas two parameters κ and ζ were needed in the constrained junction theory.

The treatment of constraints in the present study is fundamentally different than that of the tube models[19-21] which have gained widespread popularity in recent years. According to the present treatment, the constraints are assumed to localize the fluctuations of the mass centers of network chains. According to tube models, the constraints are assumed specifically to impede the fluctuations of the n Gaussian subchains of the network chain. The difference between the present model and tube models can easily be seen in the limit of infinitely strong constraints. According to the present model, the instantaneous mass centers of network chains transform affinely when constraints are infinitely strong. The modulus in this limit is obtained from eq 49 as $3[f^*]_{ph}$ for a tetrafunctional network. According to the tube models, however, the endpoints of the n Gaussian subchains would transform affinely in this limit, leading to a modulus that is n times that of the affine network model.

For both the present and the constrained junction treatments, quantitative comparison with experimentally observed moduli requires the additional knowledge of the cross-link density depicted by the cycle rank ξ. Consequently, the present theory involves two parameters (ξ, κ_G) instead of three (ξ, κ, ζ) for the constrained junction model.

Acknowledgment. B.E. gratefully acknowledges financial support by Le Ministère de la Recherche et de l'Enseignement Supérieur, France.

References and Notes

(1) James, H. M. *J. Chem. Phys.* **1947**, *15*, 651.
(2) James, H. M.; Guth, E. *J. Chem. Phys.* **1947**, *15*, 669.
(3) Graessley, W. W. *Macromolecules* **1975**, *8*, 186.

(4) Graessley, W. W. *Macromolecules* **1975**, *8*, 865.
(5) Flory, P. J. *Proc. R. Soc. London, A* **1976**, *351*, 351.
(6) Pearson, D. S. *Macromolecules* **1977**, *10*, 696.
(7) Ullman, R. *J. Chem. Phys.* **1979**, *71*, 436.
(8) Ullman, R. *Macromolecules* **1982**, *15*, 1395.
(9) Kloczkowski, A.; Mark, J. E.; Erman, B. *Macromolecules*, in press.
(10) Erman, B.; Kloczkowski, A.; Mark, J. E. *Macromolecules*, in press.
(11) Mark, J. E.; Erman, B. *Rubberlike Elasticity. A Molecular Primer*; Wiley-Interscience: New York, 1988.
(12) Queslel, J. P.; Mark, J. E. In *Comprehensive Polymer Science*; Allen, G., Ed.; Pergamon Press, Oxford, 1988.
(13) Brotzman, R. W.; Mark, J. E. *Macromolecules* **1986**, *19*, 667.
(14) Flory, P. J. *J. Chem. Phys.* **1977**, *66*, 5720.
(15) Flory, P. J.; Erman, B. *Macromolecules* **1982**, *15*, 800.
(16) Fontaine, F.; Morland, C.; Noel, C.; Monnerie, L.; Erman, B. *Macromolecules*, companion paper in this issue.
(17) Fontaine, F.; Noel, C.; Monnerie, L.; Erman, B. *Macromolecules*, companion paper in this issue.
(18) Erman, B.; Flory, P. J. *Macromolecules* **1982**, *15*, 806.
(19) de Gennes, P.-G. *J. Phys. (Les Ulis, Fr.)* **1974**, *35*, L-133.
(20) Marucci, G. *Macromolecules* **1981**, *14*, 434.
(21) Edwards, S. F.; Vilgis, T. A. *Rep. Prog. Phys.* **1988**, *51*, 243.

Mechanical Properties of Dry and Swollen *cis*-1,4-Polyisoprene Networks in Simple Tension: Experiment and Comparison with Theory

Frederic Fontaine, Catherine Morland, Claudine Noel, and Lucien Monnerie*

Laboratoire de Physico-Chimie Structurale et Macromoléculaire, Associé au CNRS, ESPCI, 10 rue Vauquelin, 75231 Paris Cedex 05, France

Burak Erman

School of Engineering, Bogazici University, Bebek, 80815, Istanbul, Turkey.
Received July 18, 1988; Revised Manuscript Received February 2, 1989

ABSTRACT: Results of simple tension experiments on dry and swollen *cis*-1,4-polyisoprene networks are reported. Measurements were performed on various networks with different cross-link densities. To decrease the time of relaxation to equilibrium, the dry samples were swollen and deswollen with a volatile solvent after the application of each load. The dependence of the observed moduli on extension and swelling is well represented by the results of calculations according to the theory of networks with constrained chains presented in the previous paper.

Introduction

Stress–strain experiments in simple tension form a convenient way of characterizing the elastic behavior of amorphous polymeric networks. A significant degree of information on the molecular structure of a network may be obtained from the graphs of reduced force plotted in terms of reciprocal extension. Such plots, commonly referred to as the Mooney–Rivlin graphs, indicate the dependence of the reduced force on the extent of extension or swelling. The reduced force [f^*], which may be identified with the shear modulus of the network, is defined as

$$[f^*] = \frac{f v_2^{1/3}}{A_d(\alpha - \alpha^{-2})} \quad (1)$$

where f is the force acting on the sample, v_2 is the volume fraction of polymer during the experiment, A_d is the cross section of the dry sample, and α is the extension ratio defined as the ratio of the final length along the direction of stretch relative to initial undistorted, swollen length.

The reduced force shows significant decrease with extension and swelling. The observed changes in the reduced force depend also strongly on the degree of cross-linking. In the present study we report results of simple tension experiments performed on *cis*-1,4-polyisoprene (PI) networks in the dry state as well as at different degrees of swelling. We report results on networks of widely different moduli ranging from high to very low degrees of cross-linking.

Results of measurements are interpreted in terms of the molecular theory introduced in the preceding paper,[1] where fluctuations of points along network chains are assumed to be affected by entanglements. The theory is a modification of the Flory theory[2] of the constrained junction model and seems to show satisfactory agreement with the data on polyisoprene networks.

Experimental Section

Samples were generously provided by Manufacture Française des Pneumatiques Michelin. Precursor polymer was an anionic commercial PI (Shell IR 307) with a high *cis*-1,4 configuration (92% cis, 5% trans, 3% 1, 2) and T_g (DSC) = −60 °C. The precursor, with a number-average molecular weight $\bar{M}_n$ = 330 000, was mixed in bulk with several amounts of pure dicumyl peroxide (DCP), molded, and cured. Curing conditions (30 min at 170 °C) were chosen to ensure full decomposition of the peroxide with negligible chain scission during curing.

The thickness t of each isotropic unswollen sample was accurately measured ($t \pm 0.001$ mm) with a Bertin micrometer (2520/D), and the length ($l \pm 0.01$ mm) was determined with a Schlumberger cathetometer (PTI ref 2207-840 9999) by measuring the distance between two points placed approximately 3 cm apart on the surface of the sample in the reference state.

Samples (dimensions ca. 100, 10, 1 mm) were first fixed at the upper clamp for at least 12 h to allow the determination of the swollen unloaded length l_0 in a state as close as possible to equilibrium. Measurements were performed by applying different dead weights at the lower end of the samples and measuring the final length l after at least 5 h. The extension α was calculated for each loading as the ratio of the final length to the initial swollen length. For experiments in the unswollen state, samples were swollen and deswollen with cyclohexane following the application of the dead load. This procedure recommended several years ago by Gee[3] decreases the time required for reaching equilibrium. Dodecane was used as the solvent for other experiments, and the volume fraction of polymer was verified not to change more than

0024-9297/89/2222-3348$01.50/0